MAGNON BEC AT ROOM TEMPERATURE
AND ITS SPATIO-TEMPORAL DYNAMICS

S. O. Demokritov[*]

Institute for Applied Physics and Center for NanoTechnology, University of Muenster
48149, Muenster, Germany

Contribution for the JETP special issue in honor of A. S. Borovik-Pomanov's 100th anniversary

Bose–Einstein condensation (BEC), predicted in 1925 by Einstein describes a formation of a collective quantum state bosons. In fact, in a gas of noninteracting bosons the thermal equilibrium distribution of particles over their energies ε is

$$n(\varepsilon) = \left[\exp\left(\frac{\varepsilon - \mu}{k_B T}\right) - 1\right]^{-1}, \qquad (1)$$

where ε is the energy of the particle, T is the temperature, k_B is the Boltzmann constant, and μ is the chemical potential of the gas, grows with growing density of the particles. It is seen from Eq. (1) that μ cannot be larger than the minimum energy of the particles ε_{min}. Correspondingly, there exist a critical density N_c:

$$N_c(T) = \left(k_B T \frac{m}{3.31\hbar^2}\right)^{3/2}, \qquad (2)$$

where m is the boson mass. If the density is larger than N_c, the gas is spontaneously divided into two fractions: particles with the density N_c distributed according to Eq. (1) and particles accumulated in the ground state. The latter fraction represents BEC [1]. Experimentally, BEC was observed in diluted atomic alkali gases at ultra-low temperatures of 10^{-7} K [2,3].

It is very straightforward idea to observe BEC in gases of quasi-particles since in this case such ultra-low temperatures are not needed, because: (i) the effective mass of quasi-particles can be essentially smaller than that of atoms; (ii) a large number of quasi-particles exists at non-zero temperatures due to thermal fluctuations; (iii) if necessary, the density of quasi-particles

can be controlled using microwave pumping [4] or illumination with light [5].

To observe BEC of magnons, we took advantage of monocrystalline films of yttrium iron garnet $Y_3Fe_2(FeO_4)_3$ (YIG) [6]. An intense electromagnetic pumping field was applied to YIG film with the thickness of 5 μm placed into a spatially uniform static magnetic field H_0 oriented in the film plane. As a result, a lot of primary parametrically pumped magnons were injected in YIG. The distribution of magnons over frequencies was studied using the time- and space-resolved Brillouin light scattering (BLS) spectroscopy [7,8]. The measured BLS intensity $I(f)$ is proportional to the reduced spectral density of magnons, $I(f) \propto \tilde{D}(f)n(f)$, where $\tilde{D}(f)$ is the density of magnon states taking into account only the magnons accessible for BLS and $n(f)$ is the magnon occupation function. Calculating $\tilde{D}(f)$ from the known magnon spectrum, the measured BLS intensity gives directly $n(f)$.

The BLS spectra recorded at different delay times with respect of start of the pumping are shown in Fig. 1. At small delay times, the data can be nicely fitted by Eq. (1) with μ being the fit parameter. One observes that the maximum value $\mu/h = f_{min} = 2.10$ GHz is reached already after 300 ns, the corresponding distribution can be considered as the critical distribution $n_c(f)$. Further increase of the density of the pumped magnons leads to BEC of magnons: magnons are collected at ε_{min} without changing the population of the states with higher frequencies as illustrated by the right-hand part of Fig. 1, showing the high-frequency parts of the magnon distribution. This part excludes a higher temperature for BLS spectra for $t > 300$ ns since variation of temperature varies magnon popula-

_____
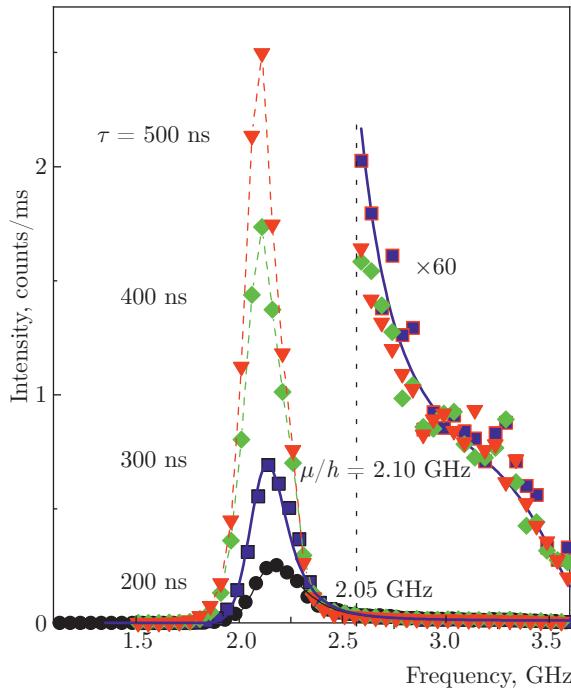[*] E-mail: demokrit@ uni-muenster.de

Fig. 1. (Color online) BLS spectra from pumped magnons at different delay times as indicated. Solid lines show the results of the fit of the spectra based on the Bose–Einstein statistics with the chemical potential being a fit parameter. Note that the critical value of the chemical potential is reached at 300 ns. The high-frequency part of the same spectrum is shown on the right

Fig. 2. (Color online) Measured two-dimensional spatial map of the BLS intensity proportional to the condensate density obtained at the maximum used pumping power. Dashed circles show the positions of topological defects in the standing-wave pattern

tions at all frequencies. The difference between a distribution at a given time t>300 ns and the critical one is non-zero in the region close to f_{min}, the width of the region $\Delta f \approx 0.3$ GHz being defined by the resolution of the spectrometer. Later experiments with the ultimate resolution have shown that the intrinsic width of the region is about 700 kHz [9], which corresponds to a high degree of coherence of the condensate, giving $\Delta f < 10^{-6} k_B T/h$.

Since the lowest-energy magnon state in in-plane magnetized magnetic films is doubly degenerate, the condensation occurs at two non-zero values of the wave vector $k = \pm k_{min} = \pm k_{BEC}$. Correspondingly, the condensate comprises two spatially overlapping wave functions ψ_+ and ψ_-. Interference of two wave functions with the opposite wave vectors should lead to a standing wave of the condensate density in the real space, provided they are phase-locked to each other. Figure 2 illustrating a two-dimensional mapping of the condensate density, clearly demonstrates a periodic pattern along the direction of the static magnetic field created as a result of such interference. The detected
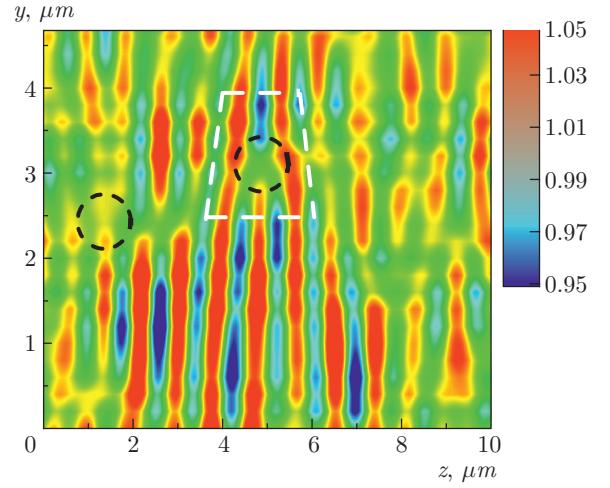
periodic modulation of the condensate density clearly confirms the existence of two spatially coherent wave functions in the magnon condensate. Moreover, the presence of topological defects marked by dashed circles is seen in Fig. 2. These defects correspond to singularities of the phase of the individual components ψ_+ and ψ_-.

To investigate second sound in magnon gas, we added to the setup a control strip line. This line allows to create an additional spatially inhomogeneous magnetic field ΔH induced by an electric current flowing in the line. If radio-frequency current flows through the control line, it causes a periodic oscillation of the magnon density underneath of the control line, which excites waves of magnon density propagating away from the control line, as shown in Fig. 3, obtained by sweeping the laser beam away from the control line, and using the time- and space-resolved BLS spectroscopy. The color code in Fig. 3 reflects the magnon density, with red/blue color corresponding to the highest/lowest density. Propagating waves of the magnon density are indicated by straight lines of the constant density in Fig. 3, with the slope of the lines being proportional to the phase velocity of the waves. By varying the frequency of the exciting signal, we were able to measure the dispersion of the second sound, which was analyzed using a corresponding theoretical model [10].

The magnon BEC takes place at the states, where the phase velocity is rather large, the magnon group velocity at the ground state is zero. Therefore, the
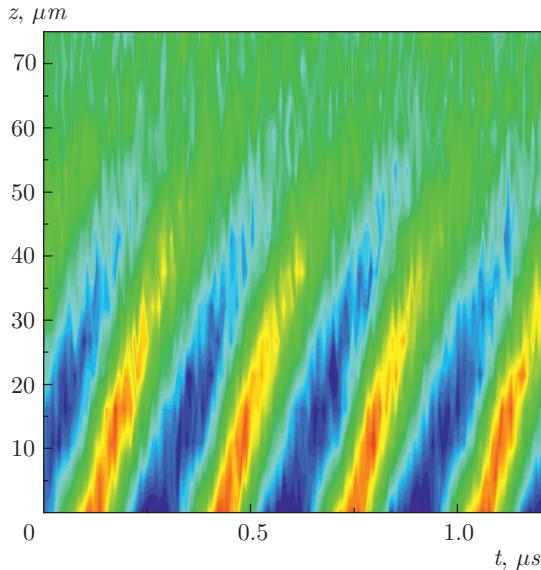
Fig. 3. (Color online) Spatio-temporal map (t is time from the start of the radio-frequency signal, z is the distance from the control line) of the measured BLS intensity for the thermalized magnon gas with red/blue color corresponding to the highest/lowest intensity. Inclined lines indicate propagating second sound waves

condensate cloud is at rest, if a homogeneous and time-independent magnetic field is applied. However, if one puts coherent condensate into constant-velocity motion, the propagating cloud of coherent magnons represents a pulse of magnon laser. Experimentally, we applied current in a form of rectangular pulses. By mapping the condensate density as a function of time and the distance from the center of the conductor we are able to detect condensate clouds propagating with a speed above 900 m/s.

The full text of this paper is published in the English version of JETP.

REFERENCES

1. A. Einstein, Sitzungsberg. Ber. Preuss. Akad. Wiss. **1**, 3 (1925).

2. M. H. Anderson, J. R. Ensher, M. R. Matthews et al., Science **269**, 198 (1995).

3. K. B. Davis, M.-O. Mewes, M. R. Andrews et al., Phys. Rev. Lett. **75**, 3969 (1995).

4. V. S. L'vov, *Wave Turbulence Under Parametric Excitation*, Springer-Verlag, Berlin (1994).

5. D. Hulin A. Mysyrowicz, and C. Benoit a la Guillaume, Phys. Rev. Lett. **45**, 1970 (1995).

6. B. Lax and K. J. Button, *Microwave Ferrites and Ferrimagnets*, McGraw-Hill, New York (1962).

7. S. O. Demokritov and V. E. Demidov, IEEE Trans. Mag. **44**, 6 (2008).

8. V. E. Demidov and S. O. Demokritov, IEEE Trans. Mag. **51**, 0800215 (2015).

9. O. Dzyapko, P. Nowik-Boltyk, B. Koene et al., IEEE Magnetic Lett. **7**, 3501805 (2016).

10. V. Tiberkevich, I. V. Borisenko, P. Nowik-Boltyk et al., Sci. Rep. **9**, 9063 (2019).